Applied Surface Science 258 (2012) 6831–6840

Contents lists available at SciVerse ScienceDirect

Applied Surface Science

journal homepage: www.elsevier.com/locate/apsusc

Numerical and experimental analysis of surface roughness generated by shot peening

Sara Bagherifard, Ramin Ghelichi, Mario Guagliano*

Department of Mechanical Engineering, Politecnico di Milano, Via La Masa, 1, 20156 Milano, Italy

A R T I C L E I N F O

Article history:
Received 3 February 2012
Received in revised form 16 March 2012
Accepted 17 March 2012
Available online 30 March 2012

Keywords:
Shot peening
Surface roughness
Numerical simulation

A B S T R A C T

Shot peening, apart from its various projected effects, modifies also the surface state of treated components in terms of surface irregularities. Bearing in mind that both the macroscopic and the microstructure surface characteristics strongly affect the mechanical structures' functionality, it is essential to carefully study the surface state of treated components. To assess the surface roughness evolution induced by shot peening, a 3D finite element model of the process is used to investigate surface topography alterations as a function of peening parameters and processing time.

Discrete data obtained from the numerical simulations are subsequently elaborated to calculate the conventional roughness parameters. The results obtained from the numerical simulations, correspond quite well with the roughness values measured experimentally on shot peened specimens.

It is indicated that the developed numerical model provides an efficient estimation of surface characteristics of shot peened specimens, in terms of surface roughness parameters and thus can be used to properly select the peening parameters considering the eventual surface roughness.

1. Introduction

Shot peening (SP) is a well-established surface treatment mainly aimed at enhancing the resistance of metallic components which are exposed to cyclic loadings, fretting and stress corrosion. The process consists in impacting the surface of a component by multiple high velocity shots that induce plastic deformation on the surface layer of material. The SP process basically modifies the surface and the characterizing parameters of the near surface substrate including principally elastic residual stress distribution, increased surface hardness, higher near-surface dislocation density and alternated surface topography.

Substantial changes in the surface features can have favorable effects for the functionality of the treated component or adversely, can make it more vulnerable to unexpected failure, depending on in-service condition. Here are some examples: for components that undergo fatigue loading, the surface roughness, can partially put the induced compressive residual stress field in the shade and cause reduced fatigue strength; i.e. provoking stress concentration at specific points, the surface roughness facilitates crack initiation under fatigue loading [1,2]. In some cases, it may even increase the natural scatter of the material in terms of fatigue strength [3].

Another example are the rotating parts in aircraft engines, shot peened to prevent the initiation and propagation of cracks; in their case surface roughness increase, turns up to reduce the aerodynamic efficiency on aerofoils [4].

On the other hand, the topography of roughened substrates is reported to play a beneficial role in coating adhesion, and in varied phenomena which can influence adhesion, such as droplet impact, wetting and solidification [5], thus providing the possibility of SP application also in biomechanical fields. It is also found to be favorable as regards fretting. The minute pockets that are produced on the shot peened surface through the plastic indentations, act as oil reservoirs, thus resulting in longer lubricant retention.

Considering the important role of surface roughness on performance of treated components, it is of particular scientific and technological importance to study the mechanism of surface roughening process and to estimate the profilometric details of the treated material. Numerical approaches simulating the real dynamic of the collisions seem to be cost effective and functional for surface topography evaluation. Finite element (FE) models are widely used for simulation of SP process and estimation of its effects, especially in terms of induced residual stresses; however very few models of shot peening or similar processes have focused on the development of surface roughness parameters.

Dai et al. [6] developed a FE model of surface nanocrystallization and hardening (SNH) based on the indentation of a rigid, high-velocity ball impacting an elastoplastic Al-5052 alloy surface. SNH is an innovative process aimed at grain refinement.

* Corresponding author. Tel.: +39 02 23998206; fax: +39 02 23998202.
E-mail address: mario.guagliano@polimi.it (M. Guagliano).

0169-4332/$ – see front matter © 2012 Elsevier B.V. All rights reserved.
doi:10.1016/j.apsusc.2012.03.111

Its difference with SP lies mainly in the size of used shots and the apposite mechanical device [7]. It shall be emphasized that roughness control for the obtained surface nanocrystallized material is very crucial, since in this case, the rough surface may even mask the beneficial effects of the surface microstructure in the nanoscale range [3,6]. Dai et al. [6] compared the numerical results in terms of peak to valley (PV) value, being calculated as the distance between the highest peak and the lowest valley, with the experimental data obtained from 3D non-contact optical profilometry roughness measurements. It is to be underlined that the particular process time that Dai et al. [6] used in their study, is much longer than the regular process duration for conventional SP; besides, as mentioned before, the common shot size used in SP process are normally smaller than those of SNH, thus it seems that direct application of the results obtained from SNH to the air blast shot peening (ABSP) case, would be somehow uncertain.

Later on, Klemenz et al. [8] developed a numerical method for the prediction of changes in the material state analyzing multiple shot impacts using a 3D FE model, by applying similarity mechanics. They also chose PV as the representative surface roughness parameter and studied the effects of shot diameter on roughness evolution mentioning that the roughness values increase linearly with ascending shot diameter.

Miao et al. [9] developed a 3D FE model with multiple randomly distributed shots to characterize the SP process. They presented a quantitative relationship of the roughness in terms of PV within the reference area, with respect to the number of shots. It was reported that the relative scatter in PV values increased slightly as the number of shots increased. This trend was explained mentioning that as the number of shots increases, the possibility of creating a deeper valley or a higher peak increases [9].

In another study, Majzoobi et al. [10], developed a 3D multiple impact FE model of SP and like previous analyses, chose PV value to study roughness development. In their case roughness was converged after 20 shot impacts developing a surface coverage of almost 88% (Coverage is defined as the ratio of the area covered by plastic indentation to the whole surface area treated by SP expressed in percentage). Roughness parameters estimated by the developed FE model was not matching with the experimental results and the reason was mentioned to be the differences between the experiment conditions and the numerical model [10].

In the most recent FE study on roughness induced by SP, Mylonas and Labeas [11], developed a 3D multi shot impacts model applied for calculation of particular surface parameters R_{tm}, defined as the mean of peak to valley heights, and S_m, defined as the horizontal spacing of adjacent peaks, aimed to calculate the induced geometrical stress concentration factor, K_t, based on an approach suggested by Li et al. [12]. The results were then compared to experimental analysis, and similar to previous cases, the difference between numerical and experimental results was attributed to the difference in experimental peening conditions and the FE model (50% FE surface coverage vs. experimental full coverage) [11].

In the light of this literature review, it can be mentioned that there are really few studies performed on roughness development of SP process and to the best knowledge of the authors of this article, none of the developed FE investigations, were based on or compared to experiments performed with similar SP conditions used in the FE analysis.

Moreover in all the mentioned studies, PV was selected as the representative parameter of surface roughness, probably for the simplicity of its calculation; however as also acknowledged by Miao et al. [9], PV is computed with the extreme values rather than with average quantities, thus being a very local parameter, it may not serve as a proper indicative value for surface roughness development. It is also to be mentioned that the PV value in most of the studies was not considered as the difference between the highest peak and the lowest valley within a sampling length, as it is in experimental measurements, but within the whole reference area [9,10], that makes the assumptions by some means more distant from the standard procedures of roughness assessment.

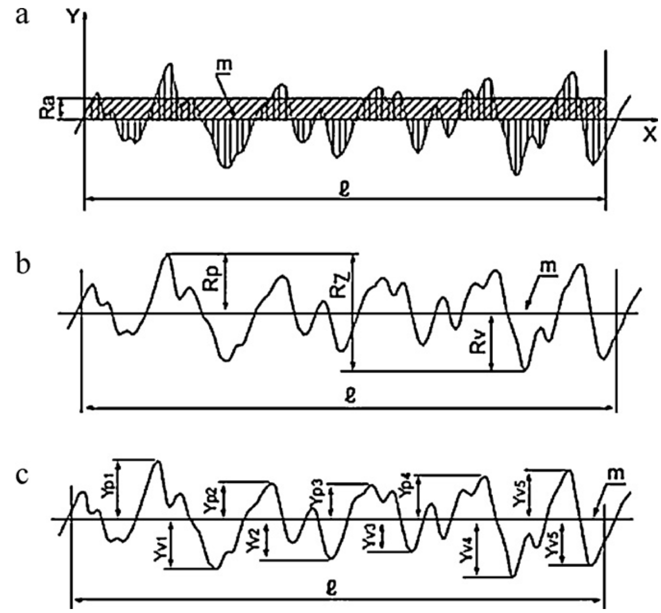

Fig. 1. Roughness parameter's representation (a) R_a; (b) R_z; (c) R_c [18,19].

Considering the aforementioned limitations of the existing studies, in the present paper, a 3D FE model of SP, developed already by the authors for the prediction of residual stresses [13], is adapted to study the roughness evolution as a function of peening parameters and processing time. A design of experiment (DOE) approach was implemented to perform different analyses using the main SP parameters including coverage, shot diameter and impact velocity, in order to predict the profilometric characteristics of the treated surface.

The roughness analysis has been realized in the sections made across the impacted area in 2D statement. The roughness parameters obtained from numerical simulation correspond quite well with the roughness values measured experimentally on steel specimens shot peened using peening parameters similar to those used in the FE analysis.

The achieved results show a good estimation of the surface characteristics of shot peened specimens. Evaluation of surface roughness via FE results is a useful tool for optimization of SP process and the proper choice of treatment parameters with a significant saving in time and cost.

2. Definition of surface roughness parameters

Surface topography is classically characterized by surface profiles obtained via electronic contact profilometry. Different roughness parameters are then extracted from the acquired surface profile. Among all the parameters for quantifying surface roughness based on tactile profile sections, R_a, the arithmetical mean deviation of the assessed profile, defined by Eq. (1), is by far the most extensive and most used parameter [14–17].

$$R_a = \frac{1}{l}\int_0^l |f(x)|dx \tag{1}$$

where $Y = f(x)$ represents the peak heights within the sampling length, l (see Fig. 1a) [18,19].

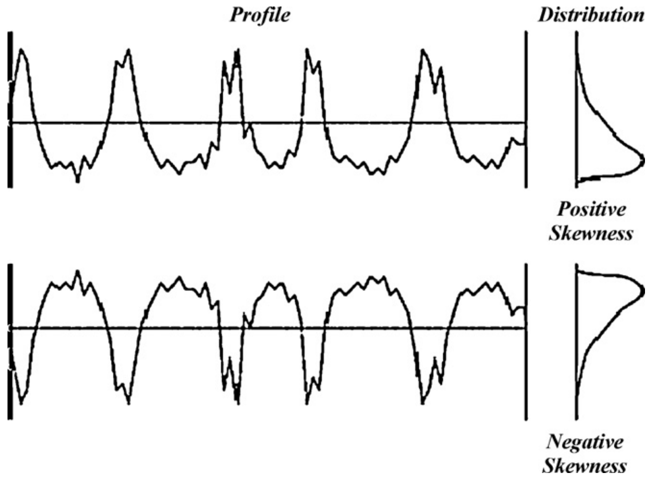

Fig. 2. Definition of skewness [21].

However, a single roughness value may not be so informative to describe the topography of a surface [17] and additional parameters shall be used to characterize the surface state.

Another well-recognized surface parameter that is commonly used in studies is R_z, maximum height of the profile, defined as sum of the largest profile peak height (R_p) and the largest profile valley depth (R_v) within a sampling length, known also as peak to valley (PV) (see Fig. 1b) [18–20]. According to its definition, R_z is an extreme characteristic value of the surface topography.

$$R_z = R_p + R_v \tag{2}$$

The other parameter chosen to be considered in this study is R_c, ten-point mean roughness, defined by Eq. (3) (see Fig. 1c) [18,19]. R_c is the arithmetic mean of the heights of the five predominant peaks and five deepest valleys, evaluated within the measurement length:

$$R_c = \frac{1}{5}\left(\sum_{i=1}^{5}|Y_p| + \sum_{i=1}^{5}|Y_v|\right) \tag{3}$$

In order to study the symmetry and peakedness of the profiles two other parameters of skewness (R_{sk}) and kurtosis (R_{ku}) have been also defined. Skewness is a measure of the symmetry of the curve describing the height distribution. A symmetrical height distribution, i.e. with as many peaks as valleys, has zero skewness. The skewness parameter can be used to distinguish between two profiles having the same R_a values but with different shapes and different height distributions, as shown in Fig. 2 [21]. The numerical formula used to calculate the skewness of a profile, which has number of points N, is as follows:

$$R_{sk} = \frac{1}{NR_q^3}\left(\sum_{i=1}^{N}Y_i^3\right) \tag{4}$$

where R_q is the root mean square (RMS) roughness parameter, which represents the standard deviation of the distribution of surface heights, and Y_i is the height of the profile at point number i.

Kurtosis represents a key feature of the height distribution, namely the 'peakedness' of the profile. A surface with a narrow height distribution, as shown in Fig. 3, has a kurtosis value greater than 3; while a surface that has a well spread out height distribution has a kurtosis value of less than 3. Fig. 3 shows these two types of kurtosis [21]. A surface with a Gaussian height distribution has a kurtosis value of 3. The kurtosis parameter numerical formula is presented in Eq. (5).

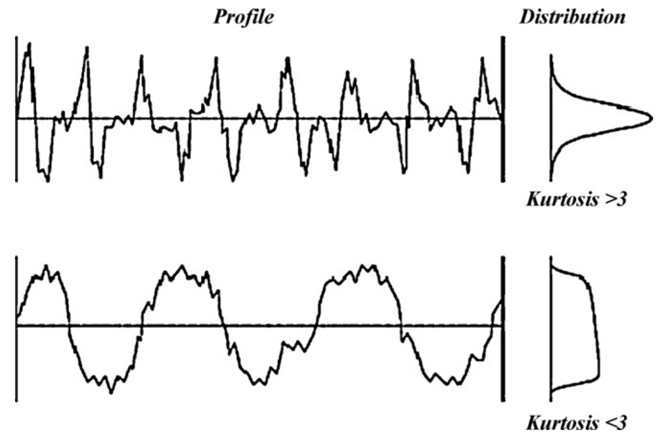

Fig. 3. Definition of kurtosis parameter [21].

$$R_{ku} = \frac{1}{NR_q^4}\left(\sum_{i=1}^{N}Y_i^4\right) \tag{5}$$

where R_q is the RMS roughness parameter and Y_i the height of the profile at point number i.

The kurtosis parameter can also be used to differentiate between surfaces, which have different shapes and have the same value of R_a. In Fig. 3, although the two profiles may have the same value of R_a, they have different shapes.

Existing standards have made just very brief citations to the surface roughness of shot peened specimens [22] and no exact measuring specifications, which consider the characteristics of shot peened surfaces, are provided [14].

Indeed, surface irregularities induced by SP process are formed by intersections of the indentations generated by each single impact. Although the shot impacts are random during the process, observations have revealed that for high surface coverage, the shot impacts are distributed on the treated surface in a relatively regular manner [14]; accordingly the mentioned standard roughness parameters, can be considered appropriate to characterize the surface topography of shot peened specimens.

3. Materials and experimental tests

Low alloy steel 39NiCrMo$_3$ (UNI EN 10083) cylindrical specimens, were subjected to different approaches of ABSP using unlike parameters. Two different set of treated specimens were considered for evaluation of the numerical model: shot peened series of SP1 and SP2; while as received not peened (NP) series were characterized to serve as reference values. Table 1 shows the applied SP parameters for each series. Cast steel shots have been used in all performed peening procedures.

Surface roughness of the treated specimens was measured and compared to that of the NP series. A Mahr profilometer PGK, that is an electronic contact instrument, equipped with MFW-250 mechanical probe and a stylus with tip radius of 2 μm was used

Table 1
Aspects of the three series of specimens.

Treatment	Shot diameter (mm)	Velocity (m/s)	Almen intensity (0.0001 in.)	Coverage %
NP	–	–	–	–
SP1	0.28	30	4–6 A	100
SP2	0.43	80	10–12 A	100

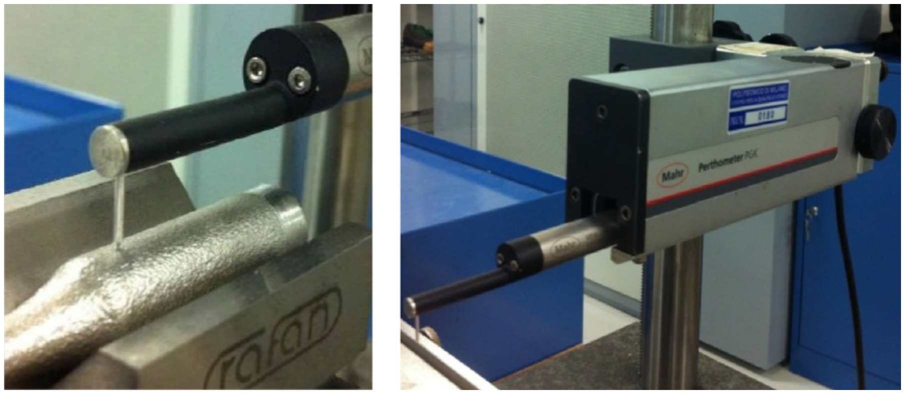

Fig. 4. Roughness measurements by means of Mahr profilometer.

to trace the surface profiles. The acquired signal was then elaborated by Mahr Perthometer Concept 5 software [23] to obtain the standard roughness parameters.

Surface roughness data were obtained by performing three measurements in three distinct areas of each individual specimen along the intersections of the surface and radial planes passing through the axis of the specimen (see Fig. 4) to consider the variability of surface roughness by location. It is to be mentioned that previous studies have revealed the independency of roughness values from the measuring direction [14]. The 2D traces were set to 4 mm long; to maintain consistency between the measurements and particularly not to excessively increase the measurement length, with respect to that of the numerical simulation.

The results indicated that the difference in the surface roughness parameters for the three locations was always found to be around 20%. Clear fluctuations of the measured roughness values on the surface of shot peened specimens, are reported also by Clausen and Stangenberg [14]. In their study all the 99 measurements showed 4–6% standard deviation from average values for R_a and R_z. This standard deviation increased up to 10% in the case of ten extreme values and became even further to 13–19.4% for R_a and 17.6–22.5% for R_z, considering four extreme values.

According to general variations, the final reported experimental surface roughness values in this study are the mean of the three performed measurements.

4. Numerical simulation

4.1. Description of FE model

A 3D model is developed to simulate the impact process using FE code Abaqus/Explicit 6.10. The target is modeled as a rectangular body and the impact area is located at the center of the upper face. All side faces are surrounded by so-called half infinite elements that provide quiet boundaries to the model avoiding the reflection of elastic shear waves [24,25]. Target mesh is set up by 513604, C3D8R 8-node linear brick elements with reduced integration and hourglass control. Nonlinear kinematic Chaboche hardening model [26] is used to model the target material. This material model does not consider the strain rate sensitivity, however previous studies have indicated that it can provide reliable results well corresponding with experimental tests [13]. Chaboche parameters for low alloy steel $39NiCrMo_3$, that is the same material used in the experiments, are presented in Table 2. Steel shots are modeled as spherical bodies consisting of tetrahedral C3D4 elements with isotropic elastic behavior. Velocity in the z-direction is defined as initial condition for all the shots, regarding an impact angle of 90°, typical for ABSP.

Table 2
Cyclic mechanical characteristic of the target material.

σ_{y0} (MPa)	E (GPa)	ν	C	γ
359.26	190	0.3	169823	501.87

For simulation of surface coverage, an exponential approach proposed by Kirk and Abyaneh [27,28] has been implemented in order to calculate the required number of impacts for obtaining the desired surface coverage. A Python subroutine has been developed to generate random impact sequence and arrangement for the shots. More details about the FE model are described in [13].

Having developed the numerical model, DOE approach is used to study the effects of different peening parameters, which determine the so-called factorial plan [29]. This strategy aims to identify quantitatively the effects of main parameters and their interaction.

The factors of the SP process and their interactions were tested by Romero et al. on the processing of aluminum alloy 2024-T351 [30] to optimize compressive residual stresses and surface hardening effects of the process, where three factors of shot type, coverage and incidence angle, were chosen to be investigated.

In the present paper, a full factorial plan with three main peening parameters including surface coverage, shot diameter and shot velocity, varying in the ranges presented in Table 3, was considered. The experimentally tested specimens, SP1 and SP2 also are in the considered ranges of peening parameters.

As affirmed also by Hirai et al. [31], the profile of the indentation is one of the basic factors influencing surface texture after SP process. Therefore in order to clarify the state of shot peened surface, the profile of the indentations produced by a single impact has been analyzed for each series of shot peened specimens, as shown in Fig. 5. The size of the induced indentation, apart from shot and target material properties, is influenced significantly also by velocity and diameter of the shots. The indentation size obtained from a single impact analysis, were compared to an analytical approach suggested by Kirk [32]. The obtained values for dimple diameter presented a difference of almost 10% compared to the results of Kirk method. However Kirk formulation is mentioned to provide a rough estimation for practical purposes, based on a simplified approach that considers few input parameters including shot diameter, shot density, shot velocity, target hardness and a coefficient of restitution, which determines how much energy is retained when

Table 3
Choice of SP parameters for DOE.

Shot diameter (mm)	0.3, 0.45, 0.6
Velocity (m/s)	30, 60, 90
Coverage %	100, 200, 300

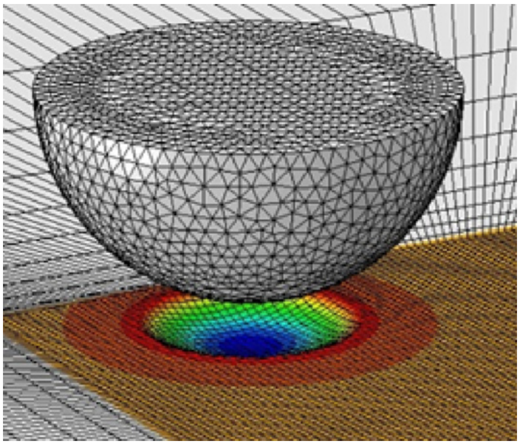

Fig. 5. The indentation induced by a single impact.

a shot bounces of a component [32]. The 10% difference can be also due to inaccuracy of the input parameters used for the analytical calculation.

After having calculated the indentation diameter for different peening parameters via FE analysis, a simple linear analytical equation has been derived for dimple diameters as a function of two input parameters that are shot velocity and shot diameter. For this purpose, the values obtained from six analyses with shot diameters of 0.3 and 0.6 mm, were used for linear regression by means of commercial software Minitab 15 [33], leaving the remaining three numerical results (for shot diameter of 0.45) to verify the obtained equation. The regression equation is:

$$d = -0.0803 + 0.00133V + 0.373D \quad (6)$$

where d stands for dimple diameter (mm), V for shot velocity (m/s) and D for shot diameter (mm). In addition, as indicator of the accuracy of the regression, R^2 = 97.5% value, representing how tight the equation fits the input data has been calculated.

Further evidence for the accuracy of Eq. (6) is provided by examining the results not regarded in the regression. Table 4 compares the values calculated by the analytical equation (Eq. (6)) and numerical analysis, which show very good correspondence.

It is to be mentioned that Eq. (6) is valid just in the case of the shot and target material used in this series of simulation. The indentation size estimation was used for mesh convergence analysis [34].

5. Model validation and calculating roughness parameters

ISO 4287 [20] is a geometrical product specification (GPS) standard that specifies terms, definitions and parameters for the determination of surface texture (roughness, waviness and primary profile) by profiling methods. It provides detailed data on surface texture, profile method terms, definitions and surface texture parameters [20]. Surface profile has been defined by this standard as the profile that results from the intersection of the real surface and a specified plane [20]. This surface profile can be categorized into three components: the high frequency or short wavelength components referred to as roughness, the medium frequencies as waviness and low frequency components as nominal form [35,36]. Fig. 6 illustrates the distinct between roughness, waviness, and nominal shape contour.

Table 4
Comparison of numerical and analytical estimations of dimple diameter.

Velocity (m/s)	Shot diameter (mm)	Numerical dimple diameter (mm)	Analytical dimple diameter, Eq. (6) (mm)	Difference (%)
90	0.45	0.205	0.207	1
60	0.45	0.173	0.167	3.5
30	0.45	0.126	0.127	0.8

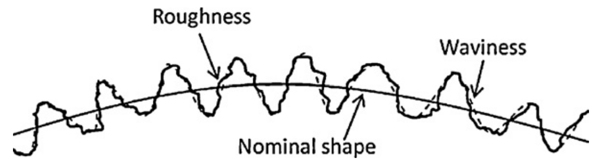

Fig. 6. Roughness and waviness profile.

A Python subroutine was prepared to extract the desired output data from the FE simulation, getting the coordinates of the nodes on the whole impact area and their assigned vertical displacement, at each time step of simulation. In this way it is possible to remodel the surface irregularities to subsequently calculate the roughness parameters step by step. Thus, another routine has been developed in Matlab software, by which the data obtained from the Python subroutine are imported to get the profile lines that are the intersection between a reference plane and the analyzed surface. This reference surface is by convention, identical to the perfect geometric surface and its location corresponds to the general direction of the real surface whose location can be identified mathematically, by the least-squares method [15]. In practice this reference line corresponds to the line that assigns equivalent path integrals for the contours positioned above and under it.

Having defined the position of the reference line, 84 profiles have been chosen to calculate the roughness parameters and finally to make an average of the obtained data. Then the filtering procedure has to be applied in order to separate different components of the surface profile. The schematic diagram of the steps is presented in Fig. 7.

There is a table of standard cutoff wavelengths in ASME B46.1-2002 [37] as well as ISO 4288-1996 [38].

ISO 4288 [38] is also a geometrical product specification (GPS) standard that specifies the rules for comparison of the measured values with the tolerance limits for surface texture parameters defined in preceding standards such as ISO 4287 [20]. It also specifies the default rules for selection of cutoff wavelength, for measuring roughness profile parameters according to IS0 4287 [20] by using stylus instruments. This standard considers a cutoff wavelength of 0.25 for the cases with a roughness evaluation length of 1.25 mm (comparable to the length considered in FE model), but at the same time attributes R_a values in the range of 0.02–0.1 mm to this evaluation length that are considerably smaller than those of the FE model and the associated experimental measurements [38]. However this cut off wavelength has been considered in the calculations.

To verify the choice of cutoff wavelength = 0.25, a visual observation was made on the deformed surface contours at the end of different analyses, without any wavelengths filtering (see Fig. 8). It is to be mentioned that in all simulations the dimensions of the impact area and consequently the zone on which the calculations have been performed are equal. It is obvious that with low velocity and small shot diameters, the target surface topography is composed of quite short wavelengths (Fig. 8a), which clearly tend to increase by increasing the shot diameter and the velocity (Fig. 8b and c). The values shown in the figure caption are representing shot diameter (mm), shot velocity (m/s) and surface coverage respectively.

In this case, the results of single impact simulations showed the maximum induced dimple diameter within the DOE series of analyses, equal to 0.27 mm. Ideally considering many adjacent dimples along the measured profile, as shown in Fig. 9, the profile's longest

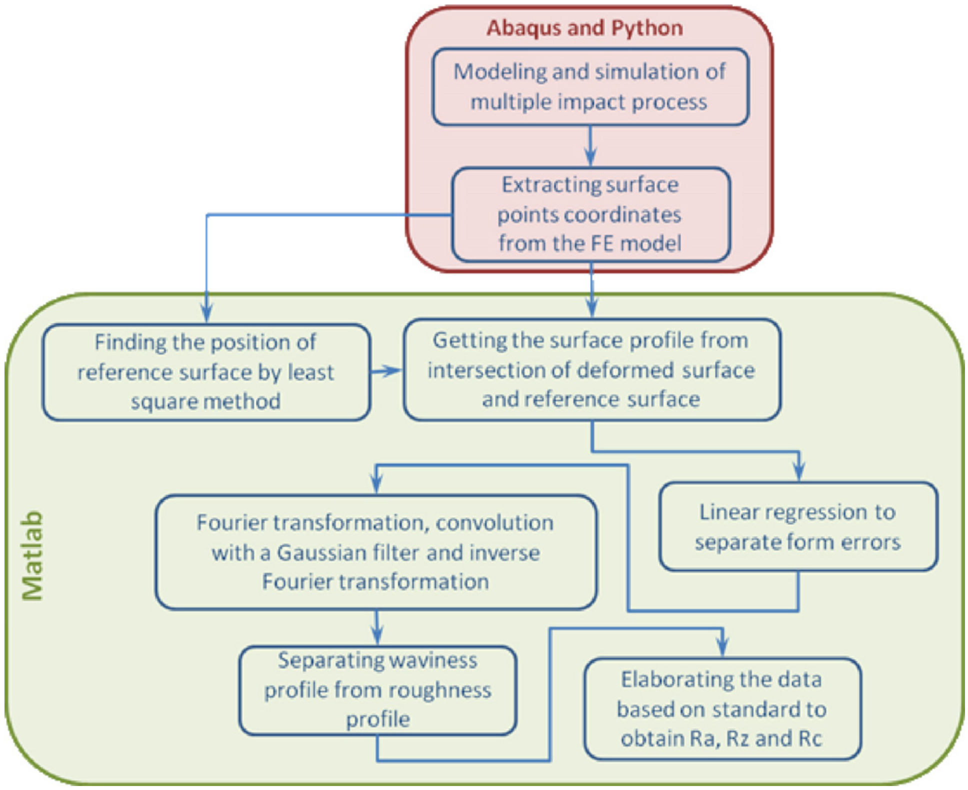

Fig. 7. Schematic diagram for roughness parameters calculation.

wavelengths cannot have a value greater than dimple diameter. The analyses were performed also by cutoff wavelength of 0.27 and negligible difference was observed compared to the results obtained by cutoff wavelength of 0.25.

The obtained data after filtering steps represents the surface irregularity without the presence of the wave component. The developed Matlab routine provides the possibility of determining the parameters R_a, R_c, R_z according to their standard definitions presented in Section 2. Indeed these indices are calculated on 84 different profiles and the output data is the average of each parameter on all the measured profiles.

The results obtained from FE simulation in case of SP1 and SP2 specimens are compared with the experimental data in Table 5. Comparison of the experimental and numerical surface roughness values shows a good correspondence. As it is observed in Table 5, the differences between experimental and numerical results apart from one case are generally less than the fluctuations of more than 20%, reported in the study performed by Clausen and Stangenberg [14]. This correspondence confirms the validity of the numerical model, highlighting the particular complexity of numerical characterization of peened surfaces. As expected, the obtained results also indicate that SP causes significantly higher surface roughness compared to as-received NP specimens. The results obtained from the DOE simulations are also presented in Table 6. The dimensions of indentations depend, in particular, on the kinetic energy of the impact, shot hardness, and the hardness of the target

Table 5
Comparison of numerical and experimental surface roughness measurements.

Specimen series	Roughness parameter	Numerical result [μm]	Experimental result [μm]	Difference (%)
NP	R_a	–	0.59	–
	R_c	–	3.20	–
	R_z	–	4.10	–
SP1	R_a	1.82	1.77	−2.7
	R_c	9.76	7.71	−21
	R_z	12.40	10.51	−15.2
SP2	R_a	4.11	4.59	+11.7
	R_c	18.15	18.68	+2.9
	R_z	28.81	29.70	+3.1

Table 6
Numerical surface roughness parameters for different peening conditions.

Coverage	Velocity [m/s]	Shot diameter [mm]	R_a [μm]	R_c [μm]	R_z [μm]
100%	30	0.3	1.51	6.83	9.64
100%	30	0.45	1.89	8.04	11.35
100%	30	0.6	2.18	9.03	13.37
100%	60	0.3	3	12.9	18.77
100%	60	0.45	3.78	15.28	22.36
100%	60	0.6	3.74	15.48	25.61
100%	90	0.3	4.34	18.34	29.06
100%	90	0.45	4.82	19.69	31.15
100%	90	0.6	5.13	21.37	37.39
200%	30	0.3	1.74	8.2	12.05
200%	30	0.45	2.17	9.65	14.19
200%	30	0.6	2.51	10.84	16.71
200%	60	0.3	3.44	15.12	22.36
200%	60	0.45	3.84	16.41	25.13
200%	60	0.6	4.29	18.69	34.44
200%	90	0.3	5.1	21.84	34.11
200%	90	0.45	6.12	26.55	43.85
200%	90	0.6	5.59	24.67	46.89
300%	30	0.3	1.96	9.56	14.46
300%	30	0.45	2.46	11.26	17.03
300%	30	0.6	2.83	12.64	20.06
300%	60	0.3	3.9	18.06	28.16
300%	60	0.45	4.46	19.92	33.02
300%	60	0.6	4.86	21.67	38.42
300%	90	0.3	5.64	25.68	43.59
300%	90	0.45	6.56	29.39	49.46
300%	90	0.6	6.54	30.47	52.55

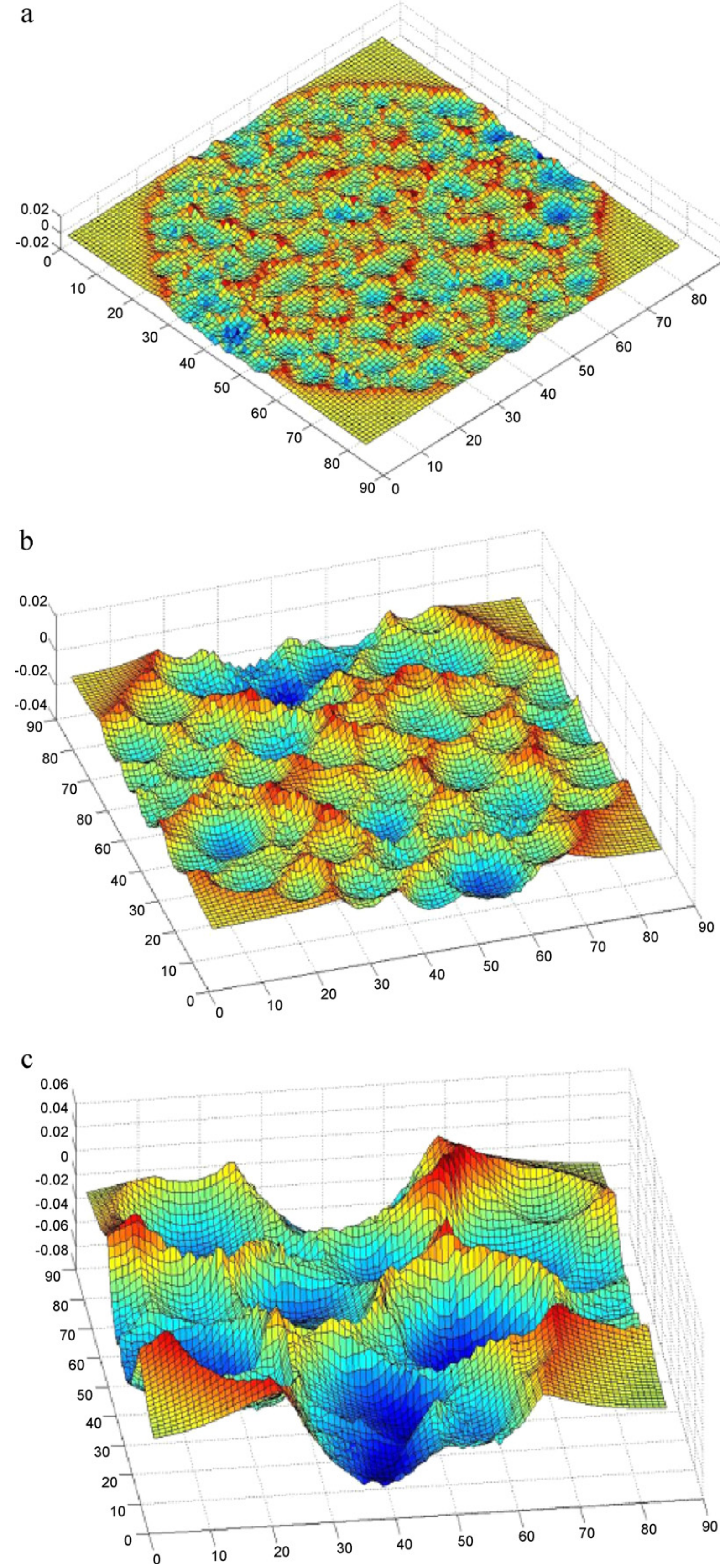

Fig. 8. View of impacted surfaces obtained from the FE analyses (a) 0.3–30–100%; (b) 0.6–30–100%; (c) 0.6–90–100% (shot diameter (mm)–shot velocity (m/s)–surface coverage).

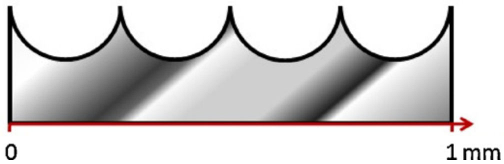

Fig. 9. Simplified profile of a shot peened surface.

material. The numerical and experimental results show a marked increase in roughness values by increasing the shot diameter and the impact velocity. These observations are confirmed also in a study performed by Bačová and Draganovskám [15].

6. Discussion

Surface roughness behavior has been studied as function of peening parameters by some researchers. Indeed, different observations have been reported about the roughness profile as function of coverage, number of impacts or processing time. Dai et al. [6] reported the roughness development for SNH to have three distinct stages, considering the PV general trend: in the ball impacting process the PV value increases initially with the processing time, due to the newly created indents and subsequently the repeated impacts in some of the valleys and ridges between indents, then decreases since there is no more flat surface for generating new indents. Furthermore, the height of the peak regions is continuously reduced, whereas the depth of the valleys will be not affected much by repeated impacts. Finally in the last phase, roughness stabilizes at a constant value as the processing time increases because the rate of generating peaks and valleys is in dynamic equilibrium with the rate of reducing the height of peaks.

However the same development route was not observed for smaller shots (5 mm vs. 7.9 mm) for which within the investigated processing time of 180 min, the roughness evolution did not enter the steady-state stage. They put forward that it took longer for the smaller indents to cover the entire plate surface for their lower impact energy. Full coverage is mentioned to be the key requirement for the PV value to start decreasing [6].

Miao et al. [9] observation on roughness development was somehow different from that of Dai et al. [6], thus divided into two main stages. During stage I, roughness increased rapidly as each impact creates an isolated indentation and independent peaks and valleys. During stage II, many indentations were superimposed so that roughness increased at a slower rate. They also established a relationship between the simulated surface roughness and the peening time which showed quite well correspondence with experimental results performed using different peening condition in terms of material and shot diameter with respect to their numerical model [9].

Majzoobi et al. [10] also confirmed the observation of Miao et al. [9] stating that roughness development consists of two stages: during stage I, roughness rises sharply as each impact creates an isolated indentation and independent peaks and valleys. During stage II, the rate of roughness increase slows down as multiple indentations due to successive shot impacts are superimposed.

In the model developed by Mylonas and Labeas [11], it is reported that the surface roughness numerically modeled with the shot patterns represents stage I of roughness development suggested by Dai et al. [6].

The development of roughness parameters as a function of coverage/number of impacts, have been studied with the proposed numerical model. The trend of surface roughness parameters for the treatment with shot diameter of 0.6 mm, shot velocity of 90 m/s and surface coverage of 300%, is presented in Fig. 10, which signifies the gradual evolution of the studied roughness parameters. Fig. 11

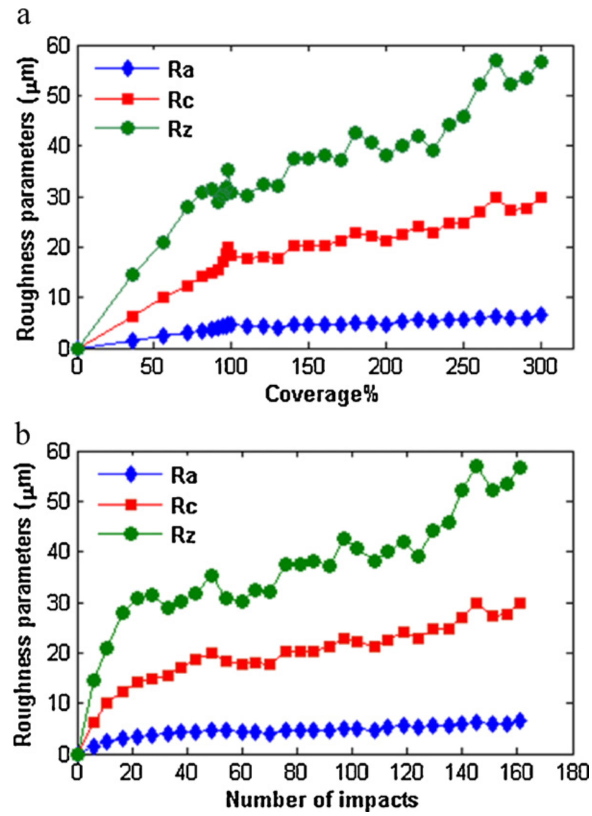

Fig. 10. Surface roughness development as a function of a. coverage b. number of impacts.

also represents the profiles of skewness and kurtosis parameters. As it can be observed in Fig. 10, the roughness parameters do not follow a certain identical trend. All the studied parameters initially increase very swiftly showing an almost linear trend up to 100% coverage, after which the increasing rate changes for each parameter. R_a tends to stabilize much earlier than the other two parameters. It reaches an almost steady state at coverage of 100% which is achieved after about 54 shots; while R_c and particularly R_z (PV), continue to rise at higher paces. It is to be underlined that the process time after which roughness parameters, tend to stabilize or decrease their rising rate, depends strongly on the peening parameters mainly shot diameter and Almen intensity that affect directly the indentation size and consequently roughness development.

The R_a profile that is quite rapidly stabilized can be explained by a similar approach to the theoretical model proposed by Kirk

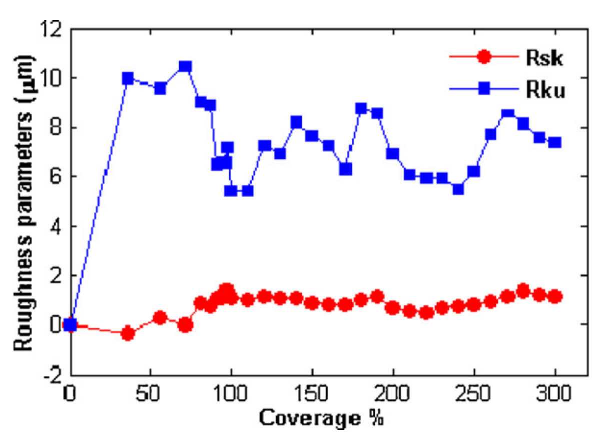

Fig. 11. Skewness and kurtosis parameters as a function of coverage.

and Abyaneh [27,28,39], and Kirk [40,41] who analyzed the theoretical basis of coverage control using Avrami equation [42,43]. In case of coverage development, they state that at the early stages, the indentations are most likely to occur without overlap so that coverage increases almost linearly with time. Later on, there will be more and more overlap of indentations. As the surface progressively becomes covered, the probability of overlap increases so that the rate of coverage decreases. Eventually when a large proportion of the area has been impacted; there remains smaller and smaller area to be covered. Hence the coverage advancement approach can be expressed exponentially [27,44].

Contemplating Kirk and Abyaneh [27,40] theoretical model for coverage, their rationalization can be applied also to roughness parameters, in this case particularly to R_a. Regarding R_c and R_z, on the other hand, the observation of Miao et al. [9] that divides roughness evolution into two main stages, seems more relevant. The first stage would be the one reported also by other researchers, which is the rapid increase in roughness parameters, and the second stage is the decrease in roughness rising rate, that in the case of this study, is more visible for R_c.

The difference between different roughness parameters can be attributed to their definitions. R_a represents mean of the heights of all peaks within the measured length, R_c corresponds to an average between ten extreme peak/valley heights, while R_z stands for maximum height of the profile that is the difference between the two extreme peak and valley. Accordingly, parameters R_c and R_z, are highly influenced by the presence of local peaks, and therefore tend to increase as the process goes on.

Thus the trend is justified by the fact that the first shots impact the target when its surface is entirely smooth, as a consequence local changes cause clear roughness increase, while as the process goes on, the changes would not be so evident as those resulting from first collisions. However local parameters as R_c and in particular R_z, continue to increase.

In case of skewness and kurtosis parameters, as shown in Fig. 11, it is observed that both parameters are more or less stabilized after 100% coverage. Even if variations particularly in terms of kurtosis are observed after full coverage, the profile is presenting a quite constant average value.

It is to be mentioned that in contact elements, positive skewness is effective in reducing fatigue failures through free abrasive erosion [45].

To come to the point, it is to be taken into account that the conventional roughness parameters are not generally accurate and as stated also by Bačová and Draganovskám [15] shall be used solely as informative quantities. They are often misrepresented by defects and other random surface errors. R_a, for example, is unable to characterize lateral roughness and to see the skewness of the profile, i.e. to distinguish between peaks and valleys [17]; R_z as an extreme parameter, is very sensitive to local imperfections and scratches that are quite common for shot peened surfaces. Therefore, as recommended also by Bačová and Draganovskám [15], to correctly evaluate the surface roughness, it is necessary to use a complex of the parameters of roughness which can reflect various specific features of the assessed surfaces, especially in case of shot peened surfaces, where the intrinsic randomness of the impacting process and its consequent local effects, impede the relative uniformity and repeatability of the surface parameters.

7. Concluding remarks

A numerical simulation has been implemented to study the development of surface roughness generated by shot peening. It consists in a finite element simulation and elaboration of the obtained data. In the light of the results the following conclusions can be drawn:

- The roughness parameters obtained from numerical simulation correspond quite well with the roughness values measured experimentally on shot peened steel specimens.
- Roughness increases with increasing shot diameter and/or shot velocity; it rises also with increasing coverage, though in this case it tends to reach a stable state, in terms of R_a, as the process time goes on. The first two dependencies are explained by larger dimensions of the generated dimples; while the changes due to coverage increase, are attributed to the greater number of impacts that modify the surface topography. These observations are confirmed also experimentally.
- A single roughness value is not so informative to describe the general surface state; additional parameters should be used in order to provide reliable data on surface topography.
- Different roughness parameters including R_a, R_c and R_z, show diverse evolution trends during the process time.
- The developed model can be used to assess the dependency of the surface roughness on various process and material parameters, providing the essential knowledge to optimize the shot peening process and consequently limit the experimental efforts and relayed costs.

References

[1] Y. Akiniwa, H. Kimura, T. Sasaki, Effect of residual stresses on fatigue strength of severely surface deformed steels by shot peening, Powder Diffr. Suppl. 24S1 (2009) 37–40.
[2] A.L. Wen, R.M. Ren, S. Wang, J.Y. Yang, Effect of surface nanocrystallization method on fatigue strength of TA2, Mater. Sci. Forum 620–622 (2009) 545–549.
[3] S. Bagherifard, M. Guagliano, Fatigue behaviour of a low-alloy steel with a nanostructured surface obtained by severe shot peening, Eng. Fract. Mech. 81 (2012) 56–68.
[4] G.G. Feldmann, W. Hennig, Th. Haubold, W.G. Zinn, B. Scholtes, Comparison of the consequences of shot peening treatment methods on the surface layer characteristics of Ti6246, Adv. Eng. Mater. 13 (9) (2011) 895–900.
[5] S. Siegmann, C.A. Brown, Surface texture correlations with tensile adhesive strength of thermally sprayed coatings using area-scale fractal analysis, in: 2nd United Thermal Spray Conference, Düsseldorf, D, 1999, pp. 355–360, ISBN/ISSN: 3-87155-653-X.
[6] K. Dai, J. Villegas, Z. Stone, L. Shaw, Finite element modeling of the surface roughness of 5052 Al, Alloy subjected to a surface severe plastic deformation process, Acta Mater. 52 (2004) 5771–5782.
[7] S. Bagheri, M. Guagliano, Review of shot peening processes to obtain nanocrystalline surfaces in metal alloys, Surf. Eng. 25 (2009) 3–14.
[8] M. Klemenz, Th. Hochrainer, L. Delonnoy, V. Schulze, O. vohringer, P. Gumbsch, Similarity rules for the shot peening process based on finite element simulations, in: International Conference of Shot Peening ICSP, vol. 9, 2005, pp. 94–99.
[9] H.Y. Miao, S. Larose, C. Perron, M. Lévesque, On the potential applications of a 3D random finite element model for the simulation of shot peening, Adv. Eng. Softw. 40 (10) (2009) 1023–1038.
[10] G.H. Majzoobi, K. Azadikhah, J. Nemati, The effects of deep rolling and shot peening on fretting fatigue resistance of Aluminum-7075-T6, Mater. Sci. Eng. A 516 (2009) 235–247.
[11] G.I. Mylonas, G. Labeas, Numerical modelling of shot peening process and corresponding products: Residual stress, surface roughness and cold work prediction, Surf. Coat. Technol. 205 (2011) 4480–4494.
[12] J.K. Li, Y. Mei, W. Duo, W. Renzhi, An analysis of stress concentrations caused by shot peening and its application in predicting fatigue strength, Fatigue Fract. Eng. Mater. Struct. 15 (12) (1992) 1271–1277.
[13] S. Bagherifard, R. Ghelichi, M. Guagliano, A numerical model of severe shot peening (SSP) to predict the generation of a nanostructured surface layer of material, Surf. Coat. Technol. 204 (24) (2010) 4081–4090.
[14] R. Clausen, J. Stangenberg, Roughness of shot-peened surfaces – definition and measurement, The 7th International Conference on Shot Peening ICSP7, Warsaw, Poland, 1999, pp. 69–77.
[15] V. Bačová, D. Draganovskám, Analyses of the quality of blasted surfaces, Mater. Sci. 40 (1) (2004) 125–131.
[16] J. Schmahling, F.A. Hamprecht, D.M.P. Hoffmann, A three-dimensional measure of surface roughness based on mathematical morphology, Int. J. Machine Tool Manuf. 46 (2006) 1764–1769.
[17] K. Anselme, P. Davidson, A.M. Popa, M. Giazzon, M. Liley, L. Ploux, Review: the interaction of cells and bacteria with surfaces structured at the nanometre scale, Acta Biomater. 6 (2010) 3824–3846.

[18] JIS B 0601: Geometrical Product Specification (GPS) – Surface Texture: Profile Method – Terms, Definitions and Surface Texture Parameters, FOREIGN STANDARD, 2001.
[19] JIS B 0031: Geometrical Product Specifications (GPS) – Indication of Surface Texture in Technical Product Documentation, Japanese STANDARD, 2003.
[20] ISO 4278: Geometrical Product Specifications (GPS) – Surface Texture: Profile Method Terms, Definitions and Surface Texture Parameters, 1st ed., 1997.
[21] E.S. Gadelmawla, M.M. Koura, T.M.A. Maksoud, I.M. Elewa, H.H. Soliman, Roughness parameters, J. Mater. Process. Technol. 123 (2002) 133–145.
[22] DIN 4762: Surface Character; Geometrical Characteristics of Surface Texture Terms, Definitions, Symbols, 1978.
[23] http://www.mahr.de (last accessed Feb. 2012).
[24] J. Schwarzer, V. Schulze, O. Vohringer, Finite element simulation of shot peening – a method to evaluate the influence of peening parameters on surface characteristics, in: Proceedings of International Conference of Shot Peening ICSP8, Munich, Germany, 2002, pp. 507–515.
[25] Abaqus Analysis User's Manual (2007), version 6.7.
[26] J. Lemaitre, J.L. Caboche, Mécanique des matériaux solides, DUNOD, Paris, 1998.
[27] D. Kirk, M.Y. Abyaneh, Theoretical basis of shot peening coverage control, in: Proceedings of the 5th International Conference on Shot Peening, 1993, pp. 183–190.
[28] D. Kirk, M.Y. Abyaneh, Theoretical basis of shot peening coverage control, Shot Peener 9 (2) (1995) 28–30.
[29] G.E.P. Box, W.G. Hunter, J.S. Hunter, Statistics for Experimenters: An Introduction to Design, Data Analysis and Model Building, John Wiley & Sons, New York, 1978.
[30] J.S. Romero, B.V. Arista, M.A.P. Rueda, R.V. Mancilla, The Taguchi Methodology Used to Determine the Factor and Interaction Effects of the Controlled Shot Peening Process, vol. 12, MFN, 2011.
[31] N. Hirai, K. Tosha, E. Rouhaud, Finite element analysis of shot peening on the form of a single dent, in: International Conference of Shot Peening ICSP9, Paris, France, 2005, pp. 82–87.
[32] D. Kirk, Peening indent dimensions, Shot Peener (2010) 24–30.
[33] http://www.minitab.com (last accessed Feb. 2012).
[34] S. Bagherifard, M. Guagliano, R. Ghelichi, Influence of mesh parameters on FE simulation of severe shot peening (SSP) aimed at generating nanocrystallized surface layer, Proc. Eng. 10 (2011) 2923–2930.
[35] J. Raja, B. Muralikrishnan, Sh. Fu, Recent advances in separation of roughness, waviness and form, Precis. Eng. 26 (2002) 222–235.
[36] M.H.A. Fadzil, E. Prakasa, H. Fitriyah, H. Nugroho, A. Mohd Affandi, S.H. Hussein, Validation on 3D surface roughness algorithm for measuring roughness of psoriasis lesion, World Acad. Sci. Eng. Technol. 63 (2010) 116–121.
[37] ASME B46.1, Surface Texture, Surface Roughness, Waviness and Lay, 2002.
[38] ISO 4288, Geometrical Product Specifications (GPS) – Surface Texture: Profile Method – Rules and Procedures for the Assessment of Surface Texture, 1996.
[39] D. Kirk, Coverage: development, measurement, control and significance, Shot Peener 16 (4) (2002) 33–36.
[40] D. Kirk, Theoretical principles of shot peening coverage, Shot Peener 19 (2) (2005) 24–26.
[41] M. Avrami, Kinetics of phase change. I. General theory, J. Chem. Phys. 7 (12) (1939) 1103–1112.
[42] M. Avrami, Kinetics of phase change. II. Transformation–time relations for random distribution of nuclei, J. Chem. Phys. 8 (2) (1940) 212–224.
[43] M. Avrami, Kinetics of phase change. III. Granulation, phase change, and microstructure, J. Chem. Phys. 9 (2) (1941) 177–184.
[44] D. Kirk, Shot peening, Aircr. Eng. Aerosp. Technol. 71 (4) (1995) 349–361.
[45] S. Kunaporn, M. Ramulu, M. Hashish, J. Hopkins, Ultra high pressure waterjet peening, part I: surface texture, in: WJTA American Waterjet Conference, Minneapolis, Minnesota, 2001.